

The complemented mutant $^{compl}\Delta Bcstc7^{niaD}$, in the STC7 of *Botrytis cinerea* led to the characterization of 11,12,13-tri-*nor*-eremophilinols derivatives

Ivonne Suárez^{a,d}, Cristina Pinedo^{a,b}, Josefina Aleu^{a,c}, Rosa Durán-Patrón^{a,c}, Antonio J. Macías-Sánchez^{a,b}, Rosario Hernández-Galán^{a,b}, Isidro G. Collado^{a,b,c,*}

^a Departamento de Química Orgánica, Facultad de Ciencias, Campus Universitario Río San Pedro s/n, Torre sur, 4^a planta, Universidad de Cádiz, 11510, Puerto Real, Cádiz, Spain

^b Instituto de Biomoléculas, Campus Universitario de Puerto Real. Universidad de Cádiz, 11510, Puerto Real, Cádiz, Spain

^c Instituto de Investigación Vitivinícola y Agroalimentaria, Campus Universitario de Puerto Real, Edificio Institutos de Investigación 2^a planta, 11510, Puerto Real, Cádiz, Spain

^d Departamento de Biomedicina y Biotecnología, Laboratorio de Microbiología, Facultad de Ciencias de Mar y Ambientales, Universidad de Cádiz, 11510, Puerto Real, Cádiz, Spain

ARTICLE INFO

Keywords:

Botrytis cinerea
Sclerotiniaceae
Phytopathogenic fungus
STC7
Eremophilinols
11,12,13-Tri-*nor*-eremophilenes
Biosynthesis

ABSTRACT

Botrytis cinerea has high potential for the production of specialized metabolites. The recent resequencing of the genome of the B05.10 strain using PacBio technology and the resulting update of the Ensembl Fungi (2017) database in the genome sequence have been instrumental in identifying new genes that could be involved in secondary metabolism. Thus, a new sesquiterpene cyclase (STC) coding gene (*Bcstc7*) has been included in the gene list from this phytopathogenic fungus. We recently constructed the null and complement transformants in STC7 which enabled us to functionally characterize this STC. Deletion of the *Bcstc7* gene abolished (+)-4-*epi*-eremophilinol biosynthesis, and could then be re-established by complementing the null mutant with the *Bcstc7* gene. Chemical analysis of the complemented transformant suggests that STC7 is the principal enzyme responsible for the key cyclization step of farnesyl diphosphate (FDP) to (+)-4-*epi*-eremophil-9-en-11-ols.

A thorough analysis of the metabolites produced by two wild-type strains, B05.10 and UCA992, and the complemented mutant $^{compl}\Delta Bcstc7^{niaD}$, revealed the isolation and structural characterization of six 11,12,13-tri-*nor*-eremophilene derivatives, in addition to a large number of known eremophilin-11-ol derivatives. The structural characterization was carried out by extensive spectroscopic techniques. The biosynthesis of these compounds is explained by a retroaldol reaction or by dehydration and oxidative cleavage of C11–C13 carbons. This is the first time that this interesting family of degraded eremophilinols has been isolated from the phytopathogenic fungus *B. cinerea*.

1. Introduction

The genus *Botrytis* (Sclerotiniaceae) is a highly diverse genus with numerous species differing in terms of their biology, ecology, morphological characteristics and host range. Fungi belonging to this genus infect all parts of the plant, including seeds, stems, leaves, flowers and fruits at the pre- and post-harvest stages (Fillinger and Elad, 2016). Currently, these fungi affect 596 genera including wild plants as well as ornamental, greenhouse and field crops such as tomatoes, vines, strawberries, tulips, and onions, among others. (Walker et al., 2016).

Without a doubt, the most common and significant species of the

genus is *Botrytis cinerea* Pers. Fr. (Sclerotiniaceae), considered the most important postharvest fungus affecting a wide range of commercial crops, including some of the most economically important ones in Spain, particularly in the region of Andalusia (Agrios et al., 2005). This fungus ranks second on the list of the ten main plant pathogenic fungi based on its scientific and economic importance (Dean et al., 2012).

This fungus infects host cells by producing toxins and reactive oxygen species and triggering oxidative bursts (Rossi et al., 2011). Two main groups of specialized metabolites (Fig. 1) are produced by *B. cinerea* (Collado and Viaud, 2016): i) sesquiterpenes such as botrydial (1) and its relatives (Colmenares et al., 2002), which are phytotoxic

* Corresponding author. Departamento de Química Orgánica, Facultad de Ciencias, Campus Universitario Río San Pedro s/n, Torre sur, 4^a planta, Universidad de Cádiz, 11510, Puerto Real, Cádiz, Spain.

E-mail address: isidro.gonzalez@uca.es (I.G. Collado).

<https://doi.org/10.1016/j.phytochem.2021.113003>

Received 14 July 2021; Received in revised form 2 November 2021; Accepted 4 November 2021

Available online 8 November 2021

0031-9422/© 2021 The Authors. Published by Elsevier Ltd. This is an open access article under the CC BY license (<http://creativecommons.org/licenses/by/4.0/>).

metabolites produced by the grey mould in soft rot regions of the infection site (Deighton et al., 2001) (Fig. 1). Also, abscisic acid (2) which mediates leaf fall in plants (Marumo et al., 1982) and a family of recently reported eremophil-9-en-11-ols (3–13) Fig. 1, which have exhibited interesting activity as effectors involved in different life cycle processes of this pathogen (Pinedo et al., 2016; Suárez et al., 2018); and ii) polyketides, mainly botcinic (14) and botcinic (15) acids and their botcinin derivatives (16, 17), the second family of toxins involved in the infection mechanism (Tani et al., 2005, 2006). Additionally, botrylactone (18), an intermediate in the biosynthesis of 14 and 15 (Moraga et al., 2011) and an interesting different group of polyketides called cinbotolides (19–21), stereochemically related to botcinins whose biological role is unknown, have been isolated from several strains of *B. cinerea* (Botubol et al., 2014; Moraga et al., 2016).

We recently reported the biosynthesis of the above-mentioned family of eremophilen-11-ol derivatives by chemical induction with copper sulphate (5 ppm) of a silent biosynthetic pathway of *B. cinerea*. As a result, a significant number of (+)-4-epieremophil-9-en-11-ol (3–13) and some 11-hydroxyeremophil-1(10)-en-2-one (22–24) were characterized and reported (Pinedo et al., 2016; Suárez et al., 2018, 2020). *In vitro* evaluation of the biological role of these metabolites indicated they were involved in the self-regulation of asexual spore production and enhanced the production of complex appressoria (infection cushions), showing for the first time that sesquiterpenoid metabolites participate in the regulation of infective structures. Furthermore, these metabolites possess an enantiomeric carbon skeleton resembling that of phytoalexin capsidiol and suggesting that this family of compounds may be effectors that inhibit plant defences or modulate plant immunity to foster the infection process (Suárez et al., 2018).

The biosynthetic pathway of these sesquiterpenes from (*E,E*)-farnesyl diphosphate (FDP) using deuterium and carbon-13 labelled acetate has been reported. Additionally, Suárez et al., 2018, 2020 have recently

identified the sesquiterpene cyclase STC7 involved in the cyclization of (*E,E*)-FDP to the germacrene intermediate (*S*)-hedycaryol, which yields (+)-4-epieremophil-9-en-11-ol derivatives via a *cis*-fused eudesmane cation.

In the course of our work focusing on the functional characterization of the sesquiterpene cyclase encoding gene *Bcstc7*, null and complemented transformants in this STC7 (Suárez et al., 2020) were fermented and studied from a metabolomic point of view. The null mutant, $\Delta Bcstc7$, halted the production of eremophilenols. However, the complemented transformant, $^{compl}\Delta Bcstc7^{niaD}$, produced a high number of compounds. In addition to polyketides derived from botcinic and botcinic acid, a large number of metabolites with an (+)-4-epieremophil-9-en-11-ol skeleton were characterized from the complemented mutant (Suárez et al., 2020). Interestingly a new family of 11,12,13-tri-*nor*-eremophilenes, which had been detected in the broth of the wild type strains B05.10 and UCA992, were produced in quantity by the complemented transformant enabling the isolation and structural characterization of this family of *nor*-sesquiterpenoids.

11,12,13-Tri-*nor*-sesquiterpenes are a rare family of metabolites isolated from different organisms. Probably the most representative and important of these *nor*-sesquiterpenes is geosmin, a tri-*nor*-eudesmane produced by many bacteria, including actinomycetes, myxobacteria, and cyanobacteria, as well as a number of eukaryotic organisms such as fungi, liverworts, insects, and plants (Gerber and Lechevalier, 1965; Schulz and Dickschat, 2007; Jiang et al., 2007). This compound is responsible for the characteristic smell of moist soil or freshly ploughed earth (Schulz and Dickschat, 2007). Although initially studies on the incorporation of labelled acetate into geosmin suggested that this bicyclic C-12 metabolite might be a degraded sesquiterpene (Spiteller et al., 2002; Bentley and Meganathan, 1981), its biosynthetic origin was later established (Dickschat et al., 2005). Thus, geosmin is generated from FDP by a bifunctional germacradienol-geosmin synthase with two

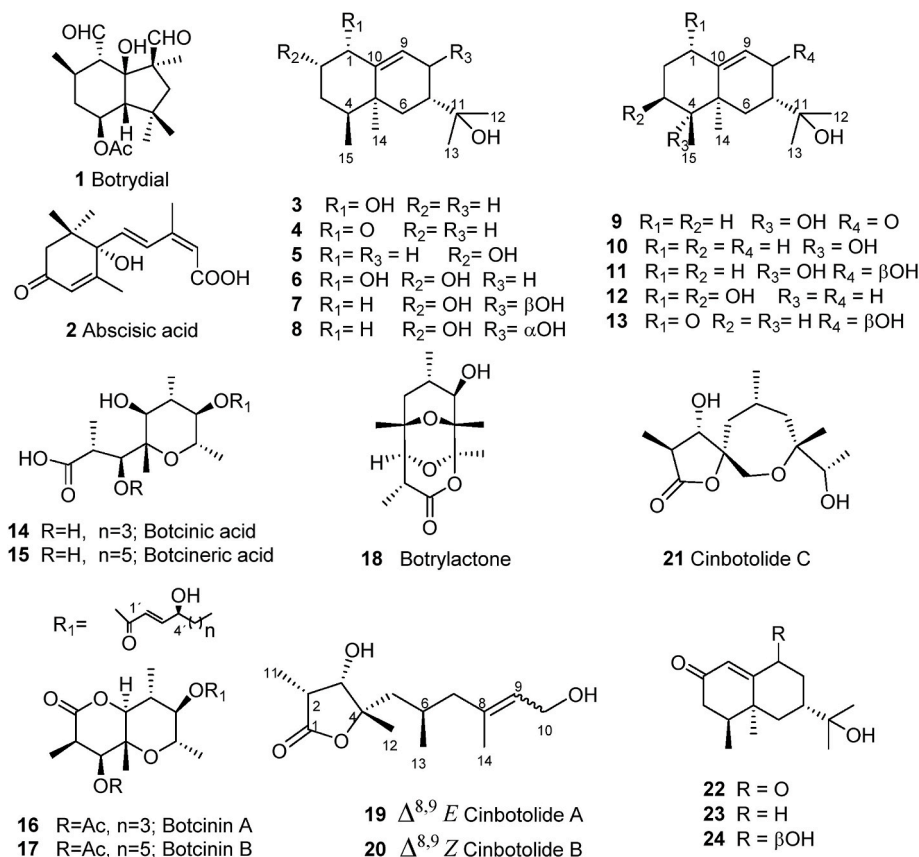


Fig. 1. Some metabolites isolated from *Botrytis cinerea*.

independent active sites with distinct catalytic functions (Jiang et al., 2007, 2008; Nawrath et al., 2008).

This paper describes a thorough comparative analysis of the metabolites produced by the wild strains B05.10 and UCA992, and the complemented mutant in the *Bcstc7* gene, *compl* Δ *Bcstc7*^{*niaD*}, which has enabled the isolation and structural characterization of six new 11,12,13-tri-*nor*-eremophilene derivatives. This family of metabolites is reported for the first time in this genus of fungi.

2. Results and discussion

Strains were incubated and fermented at 25 °C under continuous full-spectrum light (daylight), with a sub-lethal amount of copper ions, following the general procedure indicated in the experimental section. Broths were extracted with ethyl acetate and extracts chromatographed by column chromatography eluting with hexane-ethyl acetate mixtures.

Final purification of interesting fractions yielded, in addition to known compounds with botcinin structures listed in the experimental section, known eremophilenols and six new compounds with a basic skeleton of 11,12,13-tri-*nor*-eremophil-9-enols (25–30), whose structures are shown in Fig. 2. Structures were determined by extensive spectroscopic analysis using one- and two-dimensional NMR spectroscopy experiments and high-resolution mass spectrometry (HRMS). The wild-type *B. cinerea* UCA992 yielded eremophilenols 3–9, 11, 13, 22–24, and *nor*-sesquiterpenes 25, 26 and 28. The strain B05.10 yielded compounds 6, 10, 23, 25–27. Interestingly, the null mutant Δ *Bcstc7* was impaired in the production of eremophilenol derivatives whilst the complemented transformant *compl* Δ *Bcstc7*^{*niaD*} recovered the capacity to produce this family of compounds, yielding the derivatives 3–13, 22–30 (Figs. 1 and 2). In addition, the complemented transformant (Suárez et al., 2020) overproduced a higher number of compounds when compared with the wild strains B05.10 and UCA992.

The ¹H, ¹³C-NMR spectra of compounds 25–30 showed a similar pattern of signals to those of sesquiterpenes with skeleton of eremophilenols, which had lost the C₃ unit of dimethylcarbinol at C-7, as deduced from the observed twelve signals in the ¹³C-NMR, and the absence of two methyl signals in the spectrum of protons, showing a new family of 11,12,13-tri-*nor*-eremophilenols.

An important issue to settle at first is the absolute configuration of this new family of degraded eremophilanes.

The absolute configuration of (+)-4-*epi*eremophil-9-en-11-ol derivatives (3–13) was established by two ways: using the Mosher NMR method (Pinedo et al., 2016) and by chemical correlation with the enantiomeric phytoalexin capsidiol (Suárez et al., 2018), according to the article of Zhao et al., 2004. Thus, the absolute configuration and the spatial disposition of carbons C-14 and C-15 was totally established for this family of eremophilenols, C-14 axial position, C-15 equatorial

position.

A comparative of chemical shifts for C-14 (formerly C-11 in tri-*nor*-eremophilene series) between both families of compounds indicated that these were of the same order (25–30 ppm), confirming the axial position for C-11 in tri-*nor*-eremophilene series.

On the other hand, the two families of compounds ought to arise from the same biosynthetic pathway. This can be inferred from the fact that the deletion of the sesquiterpene cyclase 7 (STC 7), involved in the biosynthesis of the eremophilenols, abolished the production of eremophil-9-enols and tri-*nor*-eremophilenes, whilst the complemented transformant (Suárez et al., 2020), recovered the capacity to produce both families of compounds.

A revision about tri-*nor*-sesquiterpenes and their biosynthetic pathways has been carried out (results not published). Geosmin, as indicated in the introduction, is the unique degraded sesquiterpene biosynthesized by a bifunctional germacradienol-geosmin synthase, which causes the loss of the C₃ group in the first biosynthetic steps, by two independent active sites with distinct catalytic functions (Jiang et al., 2007, 2008; Nawrath et al., 2008).

In general, for all reported tri-*nor*-sesquiterpenes, the C-framework of degraded tri-*nor*-sesquiterpenes is generated by oxidative cleavage of the isopropenyl group with introduction of a double bond in the last step of the biosynthesis (Boland, 1993). (see 2.1 Biosynthesis of 11,12,13-tri-*nor*-eremophilenols in this manuscript).

In the case of compounds 25–30, the STC7 involved in the biosynthesis of these compounds has been reported (Suárez et al., 2020). To our knowledge, this STC has a single active site, ruling out the possibility of an independent catalytic activity involved in the loss of the dimethylcarbinol group in the first steps of biosynthesis.

From the above considerations, we can infer that the absolute configuration of the underlying carbon skeleton of tri-*nor*-eremophil-9-enols is identical to those shown by 4-*epi*eremophil-9-en-11-ol derivatives.

The ¹³C NMR spectrum of compound 25 exhibited the characteristic signal pattern of (+)-4-*epi*eremophil-9-en-11-ol, (2 quaternary carbons, 4 methines, 4 methylenes and 2 methyl groups), resembling the structure of compounds 3–13 (Fig. 1). The main differences observed were the absence of two methyl groups in the ¹H NMR and one tertiary carbon on an oxygenated function in the ¹³C NMR. This compound exhibited an ion peak in its HRMS (ESI+) at *m/z* 219.1364 [M + Na]⁺, corresponding to the formula C₁₂H₂₀O₂Na, consistent with an eremophilane skeleton which has lost the dimethylcarbinol group at C-7. As expected, compound 25 exhibited characteristic signals in its ¹H and ¹³C NMR spectra, corresponding to the trisubstituted double bond at C-9. It also exhibited a spin system in its ¹H NMR spectrum corresponding to protons attached to C-9, C-8, C-7, and C-6 (δ_{H} 5.32 (d, C=CH), 3.93 (br dd, CHOH), 3.63 (ddd, CHOH), 1.82 (CHHCHOH), and 1.41 ppm (CHHCHOH)), a singlet at δ_{H} 1.20 (CH₃), and a doublet at δ_{H} 0.98 (CHCH₃). Analysis of the COSY, HSQC and HMBC correlations (Table S1) led to the assignment shown for compound 25. Arrangement of the homoallylic/allylic dihydroxy olefinic moiety was deduced from the HMBC correlations from H-9 to C-1, C-5 and C-7; from H-7 β to C-6 and C-8; from H-6 α to C-4, C-7, C-8, C-10, and C-11; and from H-6 β to C-4, C-5, C-7, C-8, and C-10. Moreover, NOESY correlations of H-7 β with H-6 β and H-12 β , and of H-6 α with H-8 α , H-6 β , H-11 α along with those observed between H-12 β and H-3 β , H-6 β , and H-7 β , enabled us to propose stereochemistry for compound 25 as 11,12,13-tri-*nor*-4-*epi*eremophil-9-en-7 α ,8 β -diol or (4*S*,5*S*,7*R*,8*R*)-tri-*nor*-eremophil-9-en-7,8-diol.

Compounds 26 and 27 displayed a pattern of ¹H and ¹³C NMR signals that were characteristic and very similar to those of the tri-*nor*-4-*epi*eremophil-9-enol (25). Both compounds displayed characteristic signals of two methyl groups at δ_{H} 0.95 (d, *J* = 7.1 Hz) and 1.27 (s) for compound 26, and δ_{H} 0.92 (d, *J* = 7.0 Hz) and 1.23 ppm (s) for compound 27, corresponding to protons H-12 and H-11, respectively. Two methine signals at δ_{H} 3.88 (dq, *J* = 10.5, 4.8 Hz, H-7) and 3.82 ppm (br s, H-7), and 4.07 (br d, *J* = 4.1 Hz, H-8) and 4.00 ppm (br s, H-8) for compounds

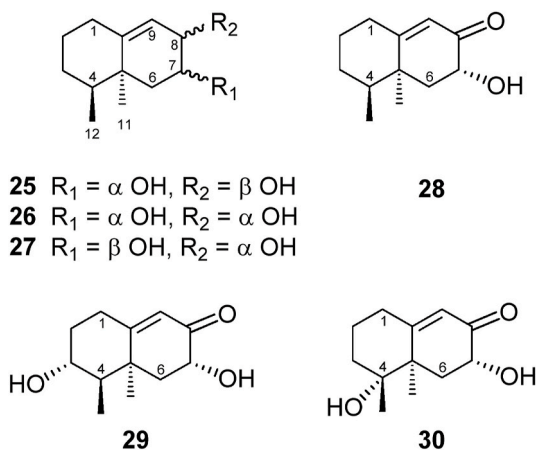


Fig. 2. New metabolites isolated from *Botrytis cinerea*.

26 and **27**, respectively, were assigned to two hydroxyl groups attached at carbons C-7 and C-8 in both compounds. Furthermore, ^1H and ^{13}C NMR spectra exhibited double-bond resonance signals at δ_{H} 5.60 ppm (H-9) for both compounds, and at δ_{C} 120.5 and 121.2 ppm (C-9), and 147.9 and 148.4 ppm (C-10), for compounds **26** and **27**, respectively, which were assigned to a trisubstituted double bond. These spectroscopic constants led us to infer that the two compounds corresponded to two diastereoisomers of compound **25**. All the carbons and their associated proton signals were assigned using COSY, HSQC and the HMBC spectra (see supporting information in Tables S2 and S3). Stereochemistry was assigned by extensive NOESY experiments. Thus, for compound **26**, irradiation of the signal H-12 β produced NOE enhancements of the signals corresponding to H-2 β , H-3 β , H-6 β and H-7 β . Irradiation of signal H-7 β produced a NOE effect at H-6 β , H-8 β and H-12 β . Correlations of H-6 β with H-7 β and H-8 β ; and of H-8 β with H-7 β and H-9 were also observed. These data, together with the large number of correlations in the HMBC experiment (Table S2), were in accord with the structure and stereochemistry shown for compound **26** as tri-*nor*-eremophil-9-en-7 α ,8 α -diol or (4*S*,5*S*,7*R*,8*S*)-tri-*nor*-eremophil-9-en-7,8-diol. NOESY experiments for compound **27** (Table S3) showed enhancement of signals H-3 β , H-4 α and H-6 β by irradiation of H-12 β ; and of signal H-11 α by irradiation of H-7, indicating the α disposition of this proton at C-7. Correlations of H-9 with H-1 β and H-8 β , and of H-8 β with H-9 were also observed. These data, along with the coupling constants of the signals corresponding to protons H-1, H-8, and H-9, which coincided with those shown in compound **26**, were consistent with the structure and stereochemistry assigned for compound **27** as tri-*nor*-4-epieremophil-9-en-7 β ,8 α -diol or (4*S*,5*S*,7*S*,8*S*)-tri-*nor*-eremophil-9-en-7,8-diol.

The ^{13}C NMR spectrum of compound **28** showed two methyl, four methylene and three methine group signals, together with those of three quaternary carbons. One of these at δ_{C} 199.8 ppm corresponded to a carbonyl group. The ^1H NMR spectrum showed, in addition to the signals for two methyl groups at δ_{H} 1.32 (s) and 1.11 ppm (d, $J = 7.2$ Hz), a pattern of signals characteristic of a (4*S*, 5*S*)-tri-*nor*-eremophileneol skeleton with one hydroxyl group. Their NMR spectra were similar to those of compound **27** that had two hydroxyl groups at C-7 and C-8. The principal differences were the presence of the signal for the carbonyl group at δ_{C} 199.8 ppm in the ^{13}C NMR spectrum, and the de-shielding of the signal assigned to H-9 at δ_{H} 5.93 ppm in the ^1H NMR spectrum. This was indicative of the presence of a $\Delta^{9,10}$ 8-keto- α,β -unsaturated ketone. This compound showed ion peaks in its HRMS (ESI+) at m/z 195.1386 and 177.1279, coinciding with the molecular formulas $\text{C}_{12}\text{H}_{19}\text{O}_2$ and $\text{C}_{12}\text{H}_{17}\text{O}$, respectively and corresponding to the pseudomolecular protonated ion and to the loss of one molecule of H_2O from a protonated molecular ion of the formula $\text{C}_{12}\text{H}_{18}\text{O}_2$. According to a basic structure of tri-*nor*-eremophileneol, it also presented a spin system in its ^1H NMR spectrum corresponding to the protons attached to C-7 and C-6 (δ_{H} 4.32 (dd, CHOH), 1.69 (CHHCHOH), and 2.31 (CHHCHOH)), a singlet at δ_{H} 1.32 ppm (CH_3), and a doublet at δ_{H} 1.11 ppm (CHCH_3). Analysis of the COSY, HSQC and HMBC correlations led to the assignment shown for compound **28**. Arrangement of the hydroxy- α,β -unsaturated ketone was deduced from the HMBC correlations of H-9 to C-1, C-5, C-7; H-7 to C-6 and C-8; H-6 α to C-4, C-5, C-7, C-8, and C-11; and from H-6 β to C-4, C-5, C-7, C-8, and C-10 (Table S4). On the other hand, NOESY correlations of H-12 β with H-7 β , H-6 β , H-4 α , and H-3 β , in addition to those of H-7 β with H-6 β and H-12 β , and H-11 α with H-1 α , H-3 α , and H-6 α , led us to assign compound **28** as (4*S*,5*S*,7*R*)-7-hydroxy-tri-*nor*-eremophil-9-en-8-one.

Compound **29** exhibited the molecular formula $\text{C}_{12}\text{H}_{18}\text{O}$, based on the ion peak at m/z 211.1334 $[\text{M} + \text{H}]^+$, and its ^1H NMR spectrum showed signals which resembled those of compound **28**, except for the presence of two signals corresponding to two protons geminal to hydroxyl groups. The ^{13}C NMR of compound **29** showed a carbonyl resonance signal at δ_{C} 199.6 ppm and resonance signals of a double bond in its NMR spectra at δ_{H} 5.97 ppm (d, H-9), and δ_{C} 121.3 (C-9) and 170.5 ppm (C-10), corresponding to a trisubstituted double bond. The two hydroxyl groups were assigned at carbons C-7 and C-3 on the basis of the

correlations observed in the HMBC experiment. Thus, there were correlations between H-7 and C-6 and C-8; H-9 and C-1, C-5, and C-7; H-4 and C-2, C-3, C-5, C-10, and C-12; H-12 and C-3, C-4, and C-5; and between H-1 β and C-2, C-3, C-5, C-9, and C-10. The position of the double bond was confirmed by the correlations previously indicated for H-9 and H-1 β , and those observed between H-11 and C-4, C-5, C-6, and C-10.

The relationship to compound **28** was supported by COSY and HSQC experiments (Table S5). The β configuration of protons H-3 and H-7 was established by the NOESY correlations observed between H-12 β and H-3, H-6 β , H-7 and H-4 α ; and between H-7 and H-6 β , C7-OH and H-12 β . Consequently, compound **29** had the structure (3*R*,4*R*,5*S*,7*R*)-3,7-dihydroxy-tri-*nor*-eremophil-9-en-8-one.

Compound **30** also showed a pattern of ^1H and ^{13}C NMR signals characteristic of a tri-*nor*-eremophileneol containing a secondary and a tertiary hydroxyl group. The compound exhibited a molecular formula $\text{C}_{12}\text{H}_{18}\text{O}_3$ based on the ion peak at m/z 211.1334 $[\text{M} + \text{H}]^+$, and possessed signals in its ^1H NMR spectrum which resembled those of compound **28**, except for the presence of two three-proton singlets instead of the singlet and doublet observed in **28**. This suggested that compound **30** had a structure corresponding to **28** with an additional hydroxyl group geminal to the methyl group at C-4. This structure was confirmed by COSY, HSQC and HMBC experiments (Table S6). The couplings observed in the HSQC and COSY spectra led to the assignment of the twelve signals observed in the ^{13}C NMR spectrum. The HMBC correlations between H-6 and C-4, C-5, C-7, C-8, C-10, and C-11; H-11 and C-4, C-5, C-6, and C-10; H-12 and C-3, C-4, and C-5; and between H-1 and C-2, C-9, and C-10, located the tertiary hydroxyl group at C-4 and the secondary hydroxyl group at C-7. The stereochemistry of the hydroxyl groups at C-4 and C-7 was assigned based on NOESY studies. Thus, irradiation of H-12 enhanced the signals corresponding to H-3 β , H-6 β , and H-7, whilst irradiation on H-7 enhanced H-6 β , H-12 β , and C7-OH, indicative of a β disposition for the methyl group at C-4. Other NOESY correlations are shown in Table S6. Consequently, compound **30** was assigned as (4*R*,5*R*,7*R*)-4,7-dihydroxy-tri-*nor*-eremophil-9-en-8-one.

2.1. Biosynthesis of 11,12,13-tri-*nor*-eremophileneols (**25–30**)

11,12,13-Tri-*nor*-sesquiterpenes are degraded sesquiterpenoids which have lost the C_3 unit of dimethylcarbinol at C-7 of the sesquiterpene skeleton. The degraded C-backbone originates from the oxidative removal of a C_3 side chain from the C_{15} sesquiterpene, which arise from farnesyl diphosphate (FDP). The C_{12} -framework is typically generated in all families of sesquiterpenes by oxidative cleavage of the C_3 substituent with the simultaneous introduction of a double bond (Boland, 1993). However, small variations of this general mechanism can be observed in different substrates or skeletons.

Based on the foregoing, the biosynthetic origin of compounds **25–30** could be explained by, a) a retroaldol reaction of eremophileneol (**A**) to give the keto derivative **B** which, after oxidation by P-450 monooxygenase at C-7, would yield the corresponding 8-keto-7-hydroxy derivatives **C** corresponding to compounds **28–30**. Subsequent reduction of carbonyl group at C-8 could yield compounds **25–27** (Fig. 3); and by b) through elimination of H_2O giving the tetrasubstituted double bond derivative **D** which is oxidized to give **E** and then reduced in both carbonyl groups to yield the dihydroxyl diastereoisomers **F** corresponding to compounds **25–27** (Fig. 3).

3. Conclusions

Deletion of the *Bcstc 7* gene (Bcin11g06510) encoding the new sesquiterpene cyclase of *Botrytis cinerea*, STC7, halted the production of compounds with an eremophilene skeleton. The complemented mutant *compl* $\Delta\text{Bcstc7}^{\text{niaD}}$ overproduced a significant number of metabolites with the aforementioned skeleton. Among them, six new 11,12,13-tri-*nor*-eremophileneols (**25–30**) were isolated and their structures characterized

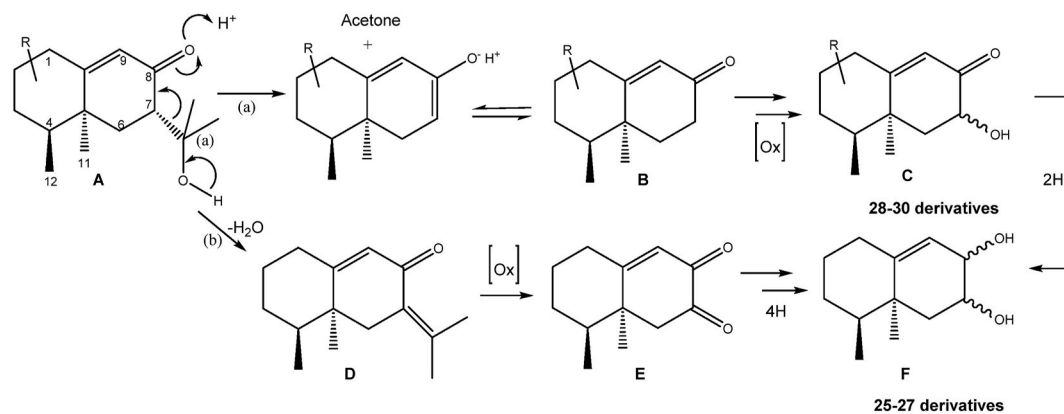


Fig. 3. Proposed mechanism for biosynthesis of compounds 25–30.

by a wide range of NMR spectroscopic analyses. Their biosynthetic origin could be explained by a retroaldol reaction or by dehydration and oxidative cleavage of C11–C13 carbons.

4. Experimental

4.1. General experimental procedures

Optical rotations were determined with a PerkinElmer 341 polarimeter. IR spectra were recorded on a PerkinElmer Spectrum BX FT-IR spectrophotometer and reported as wavenumber (cm⁻¹). ¹H and ¹³C NMR measurements were made on Agilent 500 and 600 MHz spectrometers with SiMe₄ as the internal reference. Chemical shifts were referenced to CDCl₃ (δ_H 7.25 ppm, δ_C 77.0 ppm). NMR assignments were made using a combination of 1D and 2D techniques and by comparison with those made for previously described compounds, where appropriate. High-resolution mass spectrometry (HRMS) was performed in a Q-TOF mass spectrometer in the positive-ion ESI mode. TLC was performed on Merck Kiesegel 60 F₂₅₄, 0.25 mm thick. Silica gel 60 (70–230 mesh, Merck) was used for column chromatography. HPLC was performed with a Merck-Hitachi LaChrom apparatus equipped with a UV–vis detector (L 4250) and a differential refractometer detector (RI-7490) and an Elite LaChrom-Hitachi apparatus equipped with a differential refractometer detector (RI-2490). LiChroCART LiChrospher Si 60 (5 μm, 250 mm × 4 mm) and LiChroCART LiChrospher Si 60 (10 μm, 250 mm × 10 mm) columns were used for isolation experiments.

4.2. Fungal material

Four strains of *Botrytis cinerea* Pers. Fr. (Sclerotiniaceae) were used in this study: wild type strains *B. cinerea* UCA992 and B05.10, the null mutant $\Delta Bcstc7$, and the complemented mutant *compl* $\Delta Bcstc7^{niaD}$ (Suárez et al., 2020). *B. cinerea* UCA992 was obtained from Domecq vineyard grapes and is on deposit at the University of Cádiz, Mycological Herbarium Collection (UCA). *B. cinerea* B05.10 was kindly provided by Prof. Tudzinski (Quidde et al., 1998).

For deletion of the *Bcstc7* gene (Bcin11g06510), encoding of the new STC7 enzyme and complementation of the deletion mutant, see methods and experimental in Suárez et al. (2020).

Conidial stock suspensions of all of these strains were maintained viable in 80% glycerol at –40 °C.

4.3. Media and culture conditions

The fungal strains were grown in 20 Roux culture bottles (1000 ml), each containing 150 ml of modified Czapek-Dox medium (50 g glucose, 1 g yeast extract, 1 g K₂HPO₄, 2.5 g NaNO₃, 0.5 g MgSO₄·7H₂O, 0.01 g FeSO₄·7H₂O, 0.005 g CuSO₄·5H₂O, pH 7, 1l of water). Bottles were

inoculated with 2×10^7 fresh conidia from a culture of *B. cinerea* on PDA medium and incubated for 27 days at 24–26 °C on static under day-light.

4.4. Extraction and isolation of metabolites

After 27 days of fermentation, the culture media (6 l) from each of the strains (UCA992, B05.10, $\Delta Bcstc7$, and *compl* $\Delta Bcstc7^{niaD}$) were filtered under vacuum to remove mycelium. Filtrates were saturated with NaCl and subjected to liquid-liquid extraction with ethyl acetate (x4). Organic extracts were washed with H₂O (x3) and then treated with dry Na₂SO₄ to remove water. Subsequently, the solvent was evaporated at reduced pressure to yield crude extracts as yellow oils, 250 mg from (*B. cinerea* UCA992), 500 mg (B05.10), 161 mg ($\Delta Bcstc7$), and 346 mg (*compl* $\Delta Bcstc7^{niaD}$).

The crude extracts were initially fractionated by column chromatography (CC), using solvent mixtures of increasing polarity (hexane-ethyl acetate) containing increasing percentages of ethyl acetate (10–100%). Subsequently, final purification of the different fractions was carried out by means of semipreparative HPLC: hexane-AcOEt-acetone 70:20:10, flow 2.5 ml min⁻¹.

Lastly, purified metabolites were subjected to spectroscopic analysis using 1D and 2D NMR, HRMS and IR techniques and their optical activity measured (α) for identification purposes.

4.4.1. Metabolomic analysis of *B. cinerea* strains

The null mutant $\Delta Bcstc7$ abolished the production of eremophilenes and no derivatives with eremophilene skeleton were detected.

B. cinerea UCA992 broth yielded the polyketide derivatives 14 (2.10 mg), 16 (1.95 mg) and 17 (2.20 mg) (Tani et al., 2005, 2006); the known eremophil-9-en-11-ols 3 (0.70 mg), 4 (0.50 mg), 5 (8.20 mg), 6 (1.70 mg), 7 (2.00 mg), 8 (2.00 mg), 9 (0.85 mg), 11 (1.00 mg), and 13 (1.50 mg) (Pinedo et al., 2016; Suárez et al., 2018); the 11-hydroxyeremophil-1(10)-en-2-ones 22 (1.95 mg), 23 (0.75 mg), and 24 (3.14 mg) (Suárez et al., 2020); and the new 11,12,13-tri-*nor*-eremophilenes 25 (1.20 mg), 26 (1.00 mg), and 28 (1.20 mg).

Strain B05.10 broth afforded the known compounds 14 (1.70 mg), 15 (3.50 mg), 16 (2.50 mg) (Tani et al., 2005, 2006); 6 (1.30 mg), 10 (3.14 mg), 23 (3.14 mg) (Pinedo et al., 2016; Suárez et al., 2018), and the new compounds 25 (1.14 mg), 26 (1.10 mg), and 27 (1.20 mg).

Lastly, the complemented mutant *compl* $\Delta Bcstc7^{niaD}$ yielded the known eremophilenols 3 (1.90 mg), 4 (0.35 mg), 5 (8.20 mg), 6 (1.20 mg), 7 (18.30 mg), 8 (23.40 mg), 9 (10.70 mg), 10 (31.50 mg), 11 (2.10 mg), 12 (8.50 mg), and 13 (3.20 mg) (Pinedo et al., 2016; Suárez et al., 2018); the 11-hydroxyeremophil-1(10)-en-2-ones 22 (3.00 mg), 23 (1.70 mg), and 24 (1.60 mg) (Suárez et al., 2020), and the new tri-*nor*-eremophilenes 25 (9.60 mg), 26 (1.20 mg) and 27 (1.00 mg), 28 (12.90 mg), 29 (3.30 mg), and 30 (1.30 mg).

4.4.1.1. (4*S*,5*S*,7*R*,8*R*)-tri-nor-eremophil-9-en-7,8-diol (25). Colourless oil, $[\alpha]_D^{28} -3$ (c 0.3, CHCl₃). IR ν_{\max} (cm⁻¹): 3353, 2931, 2866, 1461, 1377, 1054. ¹H NMR (500 MHz, CDCl₃): δ 0.98 (d, 3H, $J = 7.2$ Hz, H-12), 1.20 (s, 3H, H-11), 1.33 (m, 1H, H-3 β), 1.41 (dd, 1H, $J = 13.8, 12.4$ Hz, H-6 α), 1.47 (m, 1H, H-2a), 1.53 (m, 1H, H-2b), 1.63 (m, 1H, H-4 α), 1.82 (dd, 1H, $J = 13.8, 4.8$ Hz, H-6 β), 1.96 (tt, 1H, $J = 13.7, 4.5$ Hz, H-3 α), 2.01 (m, 1H, H-1 β), 2.25 (m, 1H, H-1 α), 3.63 (ddd, 1H, $J = 12.4, 7.7, 4.8$ Hz, H-7 β), 3.93 (br dd, 1H, $J = 7.7, 3.5$ Hz, H-8 β), 5.32 (s, 1H, H-9). ¹³C NMR (125 MHz, CDCl₃): δ 17.2 (q, C-12), 21.6 (t, C-2), 29.4 (t, C-3), 29.9 (q, C-11), 31.3 (t, C-1), 40.7 (s, C-5), 40.9 (d, C-4), 43.0 (t, C-6), 72.5 (d, C-7), 73.5 (d, C-8), 122.4 (d, C-9), 143.4 (s, C-10). MS (m/z): 196 (35) [M⁺], 178 [M⁺-18] (7), 163 [M⁺-18-15] (11), 152 (100), 137 (78), 123 (50). HRMS (ESI⁺) m/z calcd. for C₁₂H₂₀O₂ [M + Na]⁺ 219.1361, found 219.1364.

4.4.1.2. (4*S*,5*S*,7*R*,8*S*)-tri-nor-eremophil-9-en-7,8-diol (26). Colourless oil, $[\alpha]_D^{28} -13$ (c 0.1, CHCl₃). IR ν_{\max} (cm⁻¹): 3368, 2934, 2873, 1462, 1379, 1257, 1042, 1018. ¹H NMR (600 MHz, CDCl₃): δ 0.95 (d, 3H, $J = 7.1$ Hz, H₃-12), 1.27 (s, 3H, H₃-11), 1.31 (m, 1H, H-3 β), 1.48 (m, 1H, H-2 β), 1.58 (m, 1H, H-2 α), 1.61 (dd, 1H, $J = 13.9, 10.9$ Hz, H-6 α), 1.67 (m, 1H, H-4 α), 1.72 (dd, 1H, $J = 13.9, 4.7$ Hz, H-6 β), 1.98 (tt, 1H, $J = 13.8, 5.4$ Hz, H-3 α), 2.01 (m, 1H, H-1 β), 2.29 (tdd, 1H, $J = 13.7, 5.4, 1.8$ Hz, H-1 α), 3.88 (dq, 1H, $J = 10.2, 4.8$ Hz, H-7), 4.07 (d(br), 1H, $J = 4.1$ Hz, H-8) 5.60 (dd, 1H, $J = 5.4, 1.8$ Hz, H-9). ¹³C NMR (150 MHz, CDCl₃): δ 16.8 (q, C-12), 22.3 (t, C-2), 29.3 (t, C-3), 29.7 (q, C-11), 31.9 (t, C-1), 39.6 (t, C-6), 40.0 (s, C-5), 41.3 (d, C-4), 66.8 (d, C-7), 68.2 (d, C-8), 120.5 (d, C-9), 147.9 (s, C-10). MS (m/z): 196 (30) [M⁺], 178 [M⁺-18] (10), 163 [M⁺-18-15] (15), 152 (100). HRMS (ESI⁺) m/z calcd. for C₁₂H₂₀O₂Na [M + Na]⁺ 219.1361, found 219.1358.

4.4.1.3. (4*S*,5*S*,7*S*,8*S*)-tri-nor-eremophil-9-en-7,8-diol (27). Colourless oil, $[\alpha]_D^{27} -87$ (c 0.04, CHCl₃). IR ν_{\max} (cm⁻¹): 3400, 2930, 1462, 1379, 1053, 772. ¹H NMR (500 MHz, CDCl₃): δ 0.92 (d, 3H, $J = 7.0$ Hz, H₃-12), 1.23 (s, 3H, H₃-11), 1.25 (t, 1H, $J = 12.5$ Hz, H-6 α), 1.36 (m, 1H, H-3 β), 1.54 (m, 2H, H-2a, H-2b), 1.63 (m, 1H, H-4 α), 1.87 (t, 1H, $J = 12.5$ Hz, H-6 β), 1.98 (m, 1H, H-3 α), 2.06 (m, 1H, H-1 β), 2.20 (m, 1H, H-1 α), 3.82 (s(br), 1H, H-7), 4.00 (s(br), 1H, H-8) 5.60 (dd, 1H, $J = 5.7, 2.2$ Hz, H-9). ¹³C NMR (125 MHz, CDCl₃): δ 16.4 (q, C-12), 21.0 (t, C-2), 25.8 (q, C-11), 28.4 (t, C-3), 31.3 (t, C-1), 36.3 (t, C-6), 38.5 (d, C-4), 40.1 (s, C-5), 66.4 (d, C-8), 67.4 (d, C-7), 121.2 (d, C-9), 148.4 (s, C-10). HRMS (ESI⁺) m/z calcd. for C₁₂H₂₁O₂ [M + H]⁺ 197.1542, found 197.1559.

4.4.1.4. (4*S*,5*S*,7*R*)-7-hydroxy-tri-nor-eremophil-9-en-8-one (28). Colourless oil, $[\alpha]_D^{27} +85$ (c 0.2, CHCl₃). IR ν_{\max} (cm⁻¹): 3442, 2934, 2870, 1680, 1463, 1085, 889, 848. ¹H NMR (500 MHz, CDCl₃): δ 1.11 (dd, 3H, $J = 7.2, 0.6$ Hz, H₃-12), 1.32 (s, 3H, H₃-11), 1.40 (m, 1H, H-3 β), 1.62 (m, 1H, H-2a), 1.69 (t, 1H, $J = 13.8$ Hz, H-6 α), 1.77 (m, 1H, H-2b), 1.96 (m, 1H, H-4 α), 2.10 (tt, 1H, $J = 14.0, 4.7$ Hz, H-3 α), 2.21 (dd, 1H, $J = 13.4, 4.2, 1.9$ Hz, H-1 β), 2.31 (dd, 1H, $J = 13.8, 7.5$ Hz, H-6 β), 2.52 (tdd, 1H, $J = 13.4, 5.6, 1.9$ Hz, H-1 α), 4.32 (dd, 1H, $J = 13.3, 7.5$ Hz, H-7 β), 5.93 (d, 1H, $J = 1.9$ Hz, H-9). ¹³C NMR (125 MHz, CDCl₃): δ 17.2 (q, C-12), 22.7 (t, C-2), 29.3 (t, C-3), 30.9 (q, C-11), 33.0 (t, C-1), 41.7 (s, C-5), 43.0 (d, C-4), 43.2 (t, C-6), 69.7 (d, C-7), 121.5 (d, C-9), 170.5 (s, C-10), 199.8 (s, C-8). HRMS (ESI⁺) m/z calcd. for C₁₂H₁₉O₂ [M + H]⁺ 195.1385, found 195.1386; calcd. for C₁₂H₁₇O [M + H - H₂O]⁺ 177.1279, found 177.1279.

4.4.1.5. (3*R*,4*R*,5*S*,7*R*)-3,7-dihydroxy-tri-nor-eremophil-9-en-8-one (29). Colourless oil, $[\alpha]_D^{27} -4$ (c 0.02, CHCl₃). IR ν_{\max} (cm⁻¹): 3423, 2924, 1676, 1083, 772, 668. ¹H NMR (500 MHz, CDCl₃): δ 1.10 (d, 3H, $J = 7.4$ Hz, H₃-12), 1.56 (s, 3H, H₃-11), 1.60 (t, 1H, $J = 14.2$ Hz, H-6 α), 1.82 (m, 1H, H-2a), 1.92 (m, 1H, H-2b), 2.03 (m, 1H, H-4 α), 2.14 (ddd, 1H, $J = 13.1, 4.7, 2.6$ Hz, H-1 β), 2.36 (dd, 1H, $J = 14.2, 7.5$ Hz, H-6 β), 2.92 (tdd, 1H, $J = 13.5, 5.4, 1.8$ Hz, H-1 α), 3.56 (d, 1H, $J = 2$ Hz,

C7-OH), 3.90 (s(br), 1H, H-3), 4.29 (ddd, 1H, $J = 13.3, 7.5, 2.0$ Hz, H-7 β), 5.97 (d, 1H, $J = 1.8$ Hz, H-9). ¹³C NMR (125 MHz, CDCl₃): δ 17.1 (q, C-12), 28.2 (t, C-1), 31.0 (t, C-2), 32.4 (q, C-11), 41.3 (s, C-5), 43.0 (t, C-6), 49.8 (d, C-4), 69.5 (d, C-7), 73.2 (d, C-3), 121.3 (d, C-9), 170.5 (s, C-10), 199.6 (s, C-8). HRMS (ESI⁺) m/z calcd. for C₁₂H₁₉O₃ [M + H]⁺ 211.1334, found 211.1344.

4.4.1.6. (4*R*,5*R*,7*R*)-4,7-dihydroxy-tri-nor-eremophil-9-en-8-one (30). Colourless oil, $[\alpha]_D^{27} +29$ (c 0.02, CHCl₃). IR ν_{\max} (cm⁻¹): 3403, 2926, 1677, 1376, 1099, 771, 668. ¹H NMR (500 MHz, CDCl₃): δ 1.30 (s, 3H, H₃-11), 1.39 (s, 3H, H₃-12), 1.47 (t, 1H, $J = 14.5$ Hz, H-6 α), 1.51 (m, 1H, H-2a), 1.62 (m, 1H, H-3), 1.92 (m, 1H, H-2b), 1.99 (m, 1H, H-3), 2.23 (m, 1H, H-1 β), 2.54 (tdd, 1H, $J = 13.6, 5.8, 2$ Hz, H-1 α), 2.86 (dd, 1H, $J = 14.5, 7.6$ Hz, H-6 β), 4.37 (dd, 1H, $J = 13.7, 7.4$ Hz, H-7 β), 5.90 (d, 1H, $J = 1.9$ Hz, H-9). ¹³C NMR (125 MHz, CDCl₃): δ 23.8 (t, C-2), 25.4 (q, C-12), 26.7 (q, C-11), 32 (t, C-1), 37.6 (t, C-3), 36.7 (t, C-6), 46.6 (s, C-5), 69.9 (d, C-7), 76.4 (d, C-4), 121.5 (d, C-9), 169.9 (s, C-10), 199.3 (s, C-8). HRMS (ESI⁺) m/z calcd. for C₁₂H₁₉O₃ [M + H]⁺ 211.1334, found 211.1341.

Declaration of competing interest

The authors declare that they have no known competing financial interests or personal relationships that could have appeared to influence the work reported in this paper.

Acknowledgments

This research was supported by grants from MICINN-ERDF (RTI 2018-097356-B-C21 and -B-C22). Use of NMR facilities at the Servicio Centralizado de Ciencia y Tecnología (SCCYT) of the University of Cádiz is acknowledged.

Appendix A. Supplementary data

Supplementary data to this article can be found online at <https://doi.org/10.1016/j.phytochem.2021.113003>.

References

- Agrios, G.N., 2005. Plant Pathology, fifth ed. Elsevier Academic Press, San Diego, CA.
- Bentley, R., Meganathan, R., 1981. Geosmin and methylisoborneol biosynthesis in streptomycetes. Evidence for an isoprenoid pathway and its absence in non-differentiating isolates. FEBS Lett. 125 (2), 220–222.
- Boland, W., 1993. Oxidative bond cleavage reactions in Nature; mechanistic and ecological aspects. Pure Appl. Chem. 65 (6), 1133–1142. <https://doi.org/10.1351/pac199365061133>.
- Botubol Ares, J.M., Durán-Peña, M.J., Macías-Sánchez, A.J., Hanson, J.R., Collado, I.G., Hernández-Galán, R., 2014. The asymmetric total synthesis of cinbotolide: a revision of the original structure. J. Org. Chem. 79 (23), 11349–11358. <https://doi.org/10.1021/jo501471m>.
- Collado, I.G., Viaud, M., 2016. Secondary metabolism in *Botrytis cinerea*: combining genomic and metabolomic approaches. In: Fillingner, S., Elad, Y. (Eds.), *Botrytis – the Fungus, the Pathogen and its Management in Agricultural Systems*. Springer International Publishing, Switzerland, pp. 291–313. https://doi.org/10.1007/978-3-319-23371-0_15.
- Colmenares, A.J., Aleu, J., Durán-Patrón, R., Collado, I.G., Hernández-Galán, R., 2002. The putative role of botrydial and related metabolites in the infection mechanism of *Botrytis cinerea*. J. Chem. Ecol. 28, 997–1005. <https://doi.org/10.1023/A:1015209817830>.
- Dean, R., Van Kan, J.A.L., Pretorius, Z.A., Hammond-Kosack, K.E., Di Pietro, A., Spanu, P.D., Rudd, J.J., Dickman, M., Kahmann, R., Ellis, J., Foster, G.D., 2012. The Top 10 fungal pathogens in molecular plant pathology. Mol. Plant Pathol. 13 (4), 414–430. <https://doi.org/10.1111/j.1364-3703.2011.00783.x>.
- Deighton, N., Muckenschnabel, I., Colmenares, A.J., Collado, I.G., Williamson, B., 2001. Botrydial is produced in plant tissues infected by *Botrytis cinerea*. Phytochemistry 57, 689–692. [https://doi.org/10.1016/S0031-9422\(01\)00088-7](https://doi.org/10.1016/S0031-9422(01)00088-7).
- Dickschat, J.S., Bode, H.B., Mahmud, T., Muller, R., Schulz, S., 2005. A novel type of geosmin biosynthesis in myxobacteria. J. Org. Chem. 70, 5174–5182. <https://doi.org/10.1021/jo050449g>.
- Fillingner, S., Elad, Y., 2016. *Botrytis – the Fungus, the Pathogen and its Management in Agricultural Systems*. Springer International Publishing, Switzerland. <https://doi.org/10.1007/978-3-319-23371-0>.

- Gerber, N.N., Lechevalier, H.A., 1965. Geosmin, an earthy smelling substance isolated from actinomycetes. *Appl. Microbiol.* 13, 935–938. <https://doi.org/10.1128/aem.13.6.935-938.1965>.
- Jiang, J., He, X., Cane, D.E., 2007. Biosynthesis of the earthy odorant geosmin by a bifunctional *Streptomyces coelicolor* enzyme. *Nat. Chem. Biol.* 3 (11), 711–715. <https://doi.org/10.1038/nchembio.2007.29>.
- Jiang, J., Cane, D.E., 2008. Geosmin biosynthesis. Mechanism of the fragmentation-rearrangement in the conversion of germacadienol to geosmin. *J. Am. Chem. Soc.* 130, 428–429. <https://doi.org/10.1021/ja077792i>.
- Marumo, S., Katayama, M., Komori, E., Ozaki, Y., Natsume, M., Kondo, S., 1982. Microbial production of abscisic acid by *Botrytis cinerea*. *Agric. Biol. Chem.* 46, 1967–1968. <https://doi.org/10.1080/00021369.1982.10865367>.
- Moraga, J., Pinedo, C., Durán-Patrón, R., Collado, I.G., Hernández-Galán, R., 2011. Botrylactone: new interest in an old molecule—review of its absolute configuration and related compounds. *Tetrahedron* 67, 417–420. <https://doi.org/10.1016/j.tet.2010.11.022>.
- Moraga, J., Dalmais, B., Izquierdo-Bueno, I., Aleu, J., Hanson, J.R., Hernández-Galán, R., Viaud, M., Collado, I.G., 2016. Genetic and molecular basis of botrydial biosynthesis: connecting cytochrome P450-encoding genes to biosynthetic intermediates. *ACS Chem. Biol.* 11 (10), 2838–2846. <https://doi.org/10.1021/acschembio.6b00581>.
- Nawrath, T., Dickschat, J.S., Müller, R., Jiang, J., Cane, D.E., Schulz, S., 2008. Identification of (8*S*,9*S*,10*S*)-8,10-dimethyl-1-octalin, a key intermediate in the biosynthesis of geosmin in bacteria. *J. Am. Chem. Soc.* 130, 430–431. <https://doi.org/10.1021/ja077790y>.
- Pinedo, C., Moraga, J., Barúa, J., González-Rodríguez, V.E., Aleu, J., Durán-Patrón, R., Macías-Sánchez, A.J., Hanson, J.R., Viaud, M., Hernández-Galán, R., Garrido, C., Collado, I.G., 2016. Chemically induced cryptic sesquiterpenoids and expression of sesquiterpene cyclases in *Botrytis cinerea* revealed new sporogenic (+)-4-epieremophil-9-en-11-ols. *ACS Chem. Biol.* 11, 1391–1400. <https://doi.org/10.1021/acschembio.5b00931>.
- Quidde, T., Osbourn, A.E., Tudzynski, P., 1998. Detoxification of α -tomatine by *Botrytis cinerea*. *Physiol. Mol. Plant Pathol.* 52, 151–165. <https://doi.org/10.1006/pmpp.1998.0142>.
- Rossi, F.R., Garriz, A., Marina, M., Romero, F.M., González, M.E., Collado, I.G., Pieckenstein, F.L., 2011. The sesquiterpene botrydial produced by *Botrytis cinerea* induces the hypersensitive response on plant tissues and its action is modulated by salicylic acid and jasmonic acid signalling. *Mol. Plant Microbe Interact.* 24 (8), 888–896. <https://doi.org/10.1094/MPMI-10-10-0248>.
- Schulz, S., Dickschat, J.S., 2007. Bacterial volatiles: the smell of small organisms. *Nat. Prod. Rep.* 24, 814–842. <https://doi.org/10.1039/b507392h>.
- Spiteller, D., Jux, A., Piel, J., Boland, W., 2002. Feeding of [5,5-²H₂]-1-desoxy-d-xylulose and [4,4,6,6,6-²H₅]-mevalolactone to a geosmin-producing *streptomyces* sp. and *Fossombronia pusilla*. *Phytochemistry* 61, 827–834. [https://doi.org/10.1016/S0031-9422\(02\)00282-0](https://doi.org/10.1016/S0031-9422(02)00282-0).
- Suárez, I., da Silva Lima, G., Conti, R., Pinedo, C., Moraga, J., Barúa, J., de Oliveira, A.L., Aleu, J., Durán-Patrón, R., Macías-Sánchez, A.J., Hanson, J.R., Tallarico Pupo, M., Hernández-Galán, R., Collado, I.G., 2018. Structural and biosynthetic studies on eremophilenols related to the phytoalexin capsidiol produced by *Botrytis cinerea*. *Phytochemistry* 154, 10–18. <https://doi.org/10.1016/j.phytochem.2018.06.010>.
- Suárez, I., González-Rodríguez, V.E., Viaud, M., Garrido, C., Collado, I.G., 2020. Identification of the sesquiterpene cyclase involved in the biosynthesis of (+)-4-epieremophil-9-en-11-ol derivatives isolated from *Botrytis cinerea*. *ACS Chem. Biol.* 15, 2775–2782. <https://doi.org/10.1021/acschembio.0c00561>.
- Tani, H., Koshino, H., Sakuno, E., Nakajima, H., 2005. Botcinins A, B, C, and D, metabolites produced by *Botrytis cinerea*, and their antifungal activity against *Magnaporthe grisea*, a pathogen of rice blast disease. *J. Nat. Prod.* 68, 1768–1772. <https://doi.org/10.1021/NP0503855>.
- Tani, H., Koshino, H., Sakuno, E., Cutler, H.G., Nakajima, H., 2006. Botcinins E and F and Botcinolide from *Botrytis cinerea* and structural revision of botcinolides. *J. Nat. Prod.* 69, 722–725. <https://doi.org/10.1021/NP060071X>.
- Walker, A.S., 2016. Diversity within and between species. In: Fillinger, S., Elad, Y. (Eds.), *Botrytis – the Fungus, the Pathogen and its Management in Agricultural Systems*. Springer International Publishing, Switzerland, pp. 91–125. <https://doi.org/10.1007/978-3-319-23371-6>.
- Zhao, Y., Schenk, D.J., Takahashi, S., Chappell, J., Coates, R.M., 2004. Eremophilane sesquiterpenes from capsidiol. *J. Org. Chem.* 69, 7428–7435. <https://doi.org/10.1021/JO049058C>.